Biocompatible Polypropylene Prepared by a Combination of Melt Grafting and Surface Restructuring

Qiang Shi,[1] Jie Zhao,[1,2] Paola Stagnaro,[3] Huawei Yang,[1,2] Shifang Luan,[1] Jinghua Yin[1]

[1]*State Key Laboratory of Polymer Physics and Chemistry, Changchun Institute of Applied Chemistry, Chinese Academy of Sciences, Changchun 130022, China*
[2]*Changchun Institute of Applied Chemistry, Chinese Academy of Sciences, Changchun 130022, China*
[3]*Istituto per lo Studio delle Macromolecole, Consiglio Nazionale delle Ricerche, Via De Marini 6, Genova 16149, Italy*

Received 9 March 2011; accepted 5 December 2011
DOI 10.1002/app.36641
Published online in Wiley Online Library (wileyonlinelibrary.com).

ABSTRACT: To construct biocompatible surfaces of polypropylene (PP), poly(ethylene glycol) methyl ether methacrylate (PEGMEMA) was melt-grafted onto PP backbones; this was followed by the restructuring of the surface mircostructure of the grafted PP by water treatment. The grafted products were analyzed by Fourier transform infrared spectroscopy and ^{1}H-NMR; the surface microstructure of the graft copolymer was characterized by X-ray photoelectron spectroscopy and atomic force microscopy, and the biocompatibility was evaluated by water contact angle, protein adsorption, and platelet adhesion measurements. This study showed that highly biocompatible surfaces of PP could be obtained by a combination of melt grafting and surface restructuring techniques, and the formation of hole-with-rim patterns and the enrichment of the PEGMEMA chains on the topmost surface were the key factors for the improved biocompatibility. This work advances functionalized PP generated by melt grafting as a promising candidate for applications in blood-contact devices. © 2012 Wiley Periodicals, Inc. J Appl Polym Sci 000: 000–000, 2012

Key words: biocompatibility; graft copolymers; surfaces

INTRODUCTION

The construction of biocompatible surfaces is a pivotal requirement for medical or analytical devices that contact blood.[1–3] Such devices include catheters, blood-vessel grafts, vascular stents, artificial heart valves, and hemodialysis, hemapheresis, and oxygenator membranes.[2–4] One strategy to improve biocompatibility is surface modification with poly(ethylene glycol) (PEG), which has protein- and cell-repellent properties.[5] Traditional methods aimed at grafting PEG onto a substrate surface include covalent-bond-formation processes, such as chemical coupling reactions,[6] and plasma treatment and subsequent UV-induced graft polymerizations.[7] However, both approaches require special instruments to pregenerate the functional groups on the surfaces, followed by multistep heterogeneous reactions.[6,7] Furthermore, most studied substrates have been silicon, gold, and membranes, which are rather ideal compared to the real materials applied in blood-contacting devices.[4] A practical alternative is the direct grafting of PEG-related moieties, such as poly(ethylene glycol) methyl ether methacrylate (PEGMEMA) and poly (ethylene glycol) methyl ether acrylate, onto bulk polymers to form graft copolymers by either reactive mixing or extrusion.[7,8] Despite the commercial importance of this process, the challenge of constructing biocompatible surfaces by melt grafting remains: Graft copolymers prepared by melt grafting are random copolymers; the graft points are distributed randomly along the backbone, and the graft length is much shorter than the backbone.[9,10] Unlike block copolymers with well-defined architectures, random graft copolymers cannot self-organize into ordered microstructures on the surface.[11–15] Kinetic barriers arising from the presence of quenched disorder and architectural complexity limit the extent of long-range order in these copolymers.[14,15] The rough surface with a disordered microstructure increases the protein adsorption and platelet adhesion and results in poor biocompatibility in the graft copolymer.[16] In addition, grafted PEG-related moieties often have a higher surface energy than the polymer substrate; during film preparation by a hot press or casting, the surface rearrangement driven by a reduction in the surface energy results in the depletion of PEG-related moieties from the top layer of the surface;[17] this leads to a slight improvement in the biocompatibility on the surface.

To overcome these limitations, it is necessary to find an efficient method to restructure the surface

Correspondence to: Q. Shi (shiqiang@ciac.jl.cn) or J. Yin (yinjh@ciac.jl.cn).

Contract grant sponsor: National Natural Science Foundation of China; contract grant numbers: 50803061, 50833005, 50920105320.

© 2012 Wiley Periodicals, Inc.

and enrich the surface with grafted chains. It has been reported that graft copolymers undergo a notable restructuring by responding to the change in the contacting medium from air to water.[17] Because of a specific affinity of grafted chains for water,[5,6] water can be used to induce the grafted chains to the top layer of the surface and to order the microstructure on the surface.

In this article, we report a facile method for constructing biocompatible surfaces of polypropylene (PP) through melt grafting and water-induced surface restructuring. PP is a promising candidate for blood-contact devices because of its broad-ranging mechanical properties, ease of processing, excellent chemical resistance, nontoxicity, and low price.[18,19] However, because of a lack of polar functional groups along the polymer backbone, PP exhibits poor biocompatibility.[19] The preparation of biocompatible PP, therefore, is an ongoing challenge. In this study, PP was melt-grafted with PEGMEMA to generate PP-*g*-PEGMEMA; then, spin-coated films of PP-*g*-PEGMEMA were treated with water to restructure the nanostructure/microstructure on their surfaces. Compared to those on the surface of neat PP, the protein adsorption and platelet adhesion were substantially suppressed on these restructured surfaces of modified PP. This study is of practical significance because it showed the availability to order the structures on the surface of an intrinsically disordered graft copolymer with water and paved the way to notably improve the biocompatibility of polymers by industrial process.

EXPERIMENTAL

Materials

Pellets of a commercial PP with a weight-average molecular weight of 529 kg/mol were obtained from Panjin Ethylene Plant (Panjin, Liaoning, China). Different PEGMEMA grades (weight-average molecular weights = 300, 475, and 1100; Aldrich) were purified with an inhibitor-removing column (Aldrich). Acetone and xylene were reagent-grade products.

Grafting reactions and purification of the grafted samples

Grafting reactions of PEGMEMA onto PP were carried out in a Thermal Haake batch mixer (Karlsruhe, Germany) at a temperature of 200°C and a rotor speed of 50 rpm. The monomer concentration was in the range 1–8 wt % of the feedstock. To obtain a graft copolymer with a high grafting degree (GD) while avoiding as much as possible degradation phenomena, we used a preirradiated PP as the initiator (20 wt % of the feedstock), as described elsewhere.[18]

Several grams of raw grafted PP material (after melt grafting) were pressed into thin films with thicknesses lower than 0.1 mm with a hot press operating at 190 ± 2°C. The raw grafted PP films obtained were then extracted for at least 24 h with water at room temperature. Unreacted PEGMEMA monomer and PEGMEMA oligomers were thus removed from the film. About 1 g of the water-insoluble grafted PP material thus obtained was dissolved in 100 mL of xylene at 130°C, and the resulting solution was slowly poured into acetone; most of the grafted PP with high molecular weight precipitated. A small amount of grafted PP with a very low molecular weight, referred to as residue 1, was kept in the mother liquor and was recovered by removal of the mixture of acetone and xylene under 0.2 MPa in a vacuum oven. The precipitated grafted PP material, referred to as residue 2, was dried in a vacuum oven at 90°C for 24 h.

Characterization of the grafted PP

The grafted PP with high molecular weight (residue 2) was analyzed by Fourier transform infrared (FTIR) spectroscopy (Bio-Rad FTS-135 IR instrument, Hercules, California) at a resolution of 4 cm^{-1} and with five scans.

The grafted PP with very low molecular weight (residue 1) was analyzed by ^{1}H-NMR spectroscopy (Bruker AV400 spectrometer). ^{1}H-NMR spectra of the samples were recorded at 125°C in $C_6D_4Cl_2$ (7.260 ppm). The best conditions for the experiments were optimized at sweep width (SWH) = 4194.6 Hz, relaxation time = 8.00 s, and pulse = 90° for 6.8 μs. The typical groups, PP, —CH_3 (δ = 0.8–1.0 ppm), —CH_2— (δ = 1.0–1.5 ppm), and —CH— (δ = 1.5–1.8 ppm), were observed. The functional groups of grafted PEGMEMA were assigned as follows: —CH_2C(CH$_3$) COO— (a, a′, a″; δ = 1.9–2.5 ppm), —CH$_2$C(CH_3) COO— (b; δ = 0.9–1.0 ppm), —COO—CH_2—CH$_2$—O— (c; δ = 4.2–4.4 ppm), —COO—CH$_2$—CH_2—O— (d; δ = 3.4–3.5 ppm), —O—CH_2—CH_2—O— (d′; δ = 3.5–3.9 ppm), —O—CH$_2$—CH_2—O—CH$_3$ (e; δ = 3.7–3.9 ppm), —O—CH$_2$—CH$_2$—O—CH_3 (f; δ = 3.2–3.4 ppm), and —CH$_2$—CH(CH$_3$)COO— (g; δ = 2.5–2.7 ppm).

Sample preparation and surface restructuring

The xylene solutions of the grafted copolymers (0.2 wt %) in the temperature range from 90 to 120°C were spin-coated onto heated silicon wafers to form thin films. The film thickness was about 200 nm, as measured by an optical ellipsometer (UVISEL ER, Jobin Yvon S. A. S., Paris, France). The thin films

were then heated at 100°C in a vacuum oven for 4 h and immersed in distilled water at 60°C for 24 h. The treated films were finally dried in a vacuum oven at room temperature.

Surface characterization

The surface elemental compositions were determined by highly sensitive X-ray photoelectron spectroscopy (XPS, West Sussex, UK) with a VG Scientific ESCA MK II Thermo Avantage V 3.20 analyzer with an Al/K (binding energy ($h\nu$) = 1486.6 eV) anode mono-X-ray source. The vacuum level during XPS measurements was 2.6×10^{-9} mbar. All of the samples were carefully dried *in vacuo* before observation. Angle-dependent XPS data were collected at nominal photoelectron takeoff angles from 0 to 60°. The surface spectra were collected over the range 0–1200 eV. The atomic ratios were determined from XPS measurements.

The static water contact angles of the membranes were measured at room temperature by the sessile drop method with drop shape analysis contact angle goniometer (DSA KRUSS GMBH, Hamburg 100, Hamburg, Germany). For each sample, at least six measurements were performed.

Atomic force microscopy (AFM) observations were carried out with a SPI3800N instrument equipped with a cantilever with a bending spring constant of 40 N/m and a resonance frequency of 190 kHz (Seiko, Inc., Morioka, Japan). The film surface was characterized by standard noncontact mode scanning at 0.5 Hz from the largest area (10×10 μm^2) to the smallest area (1×1 μm^2). The data were analyzed with SPI3800N probe station software (Seiko, Inc.). All images were processed with planfitting and flattening procedures.

Protein adsorption

Bovine serum albumin (BSA) was used as the model protein to evaluate the antiprotein adsorption of the graft copolymer films in phosphate buffered saline (PBS) solution (pH 7.4). Neat PP and the spin-coated films (2×1 cm^2) of grafted PP were accurately weighted and immersed into the PBS solution (pH 7.4) for 12 h. The specimens were then transferred into PBS solutions containing BSA (1.0 and 2.0 mg/mL) to incubate at 37°C for 2 h. Each sample was rinsed five times in the fresh PBS solution by gentle shaking and were then transferred into a well-plate filled with 2.5 mL of PBS solution containing 1 wt % sodium dodecyl sulfate; the protein adsorbed on the surface was then completely desorbed by sonication for 20 min. On the basis of the bicinchoninic acid method, a microbicinchoninic acid protein assay reagent kit was used to determine the concentration of the protein in the sodium dodecyl sulfate solution. The BSA concentrations were determined on the basis of the absorption at 570 nm with a TECAN ultraviolet–visible spectrometer (TECAN GENIOS, Grödig, Austria).[19] The reported data are the mean values of three different specimens for each film.

Platelet adhesion

The spin-coated films (2×1 cm^2) were placed in a tissue culture plate. Then, 20 μL of fresh platelet-rich plasma was dropped onto the center of the membrane and incubated for 60 min at 37°C. After the membranes were washed with PBS solution (pH 7.4), the platelets adhered on the film were fixed by treatment with 2.5 wt % glutaraldehyde in PBS at 4°C for 10 h. Finally, the films were washed several times with the PBS solution and dehydrated with a series of ethanol/water mixtures (30, 50, 70, 90, and 100 vol % ethanol for 30 min for each mixture).[20] The film surface was observed with field emission scanning electron microscopy (XL 30 ESEM FEG, FEI Co., Eindhoven, The Netherlands) operating at a voltage of 15 kV.

RESULTS AND DISCUSSION

Grafting reactions

The grafting reaction as a function of the reaction time is shown in Figure 1; the grafting reaction occurred after the polymer was melted, and the GD increased very rapidly in a few minutes. A slight increment in GD was observed after 5 min; this indicated that the melt-grafting reaction was fast and was almost completed in 5 min. The grafting reaction as a function of monomer concentration is shown in Figure 2. GD increased monotonously with increasing monomer concentration, reached a maximum at a monomer concentration of 6 wt % of the feedstock, and then decreased with further increases in concentration. This trend could be explained by the completion between the grafting reactions and the homopolymerization of the monomer.[18,21] Monomers with short chain lengths ($PEGMEMA_{300}$) showed the highest reactivity toward macromolecular radicals.

Characterization of PP-*g*-PEGMEMA

Figure 3 shows the representative FTIR spectra of the neat PP and purified PP-*g*-PEGMEMA (Residue 2) samples. To compare the characteristic peak intensities of each sample, the absorbance peaks were normalized by the intensity of the methyl band of PP at 898 cm^{-1}. The new peak at about 1717 cm^{-1} appearing in the grafted samples was due to

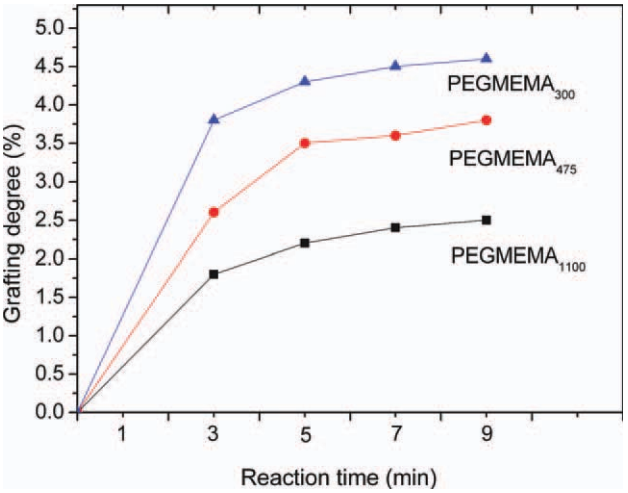

Figure 1 Grafting reactions as a function of the reaction time. [Color figure can be viewed in the online issue, which is available at wileyonlinelibrary.com.]

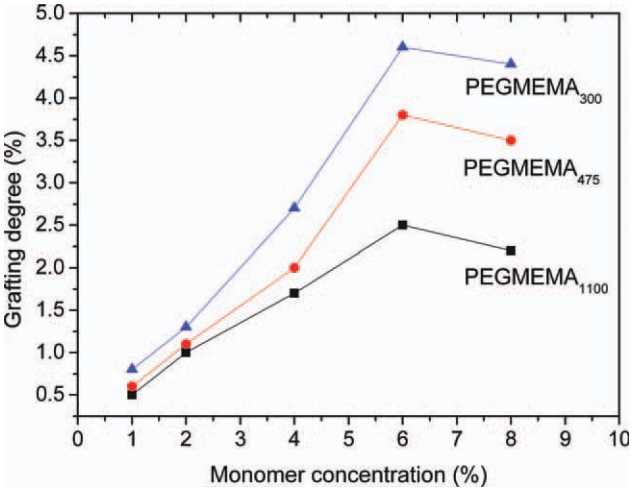

Figure 3 IR spectra of the neat and grafted PP. The absorbance peaks were normalized by the intensity of the methyl band of PP at 898 cm^{-1}. [Color figure can be viewed in the online issue, which is available at wileyonlinelibrary.com.]

carbonyl group (C=O) stretching vibrations of the grafted PEGMEMA; this provided qualitative evidence of grafting in the melt.[3] The intensity of this peak at 1717 cm^{-1} decreased with increasing chain length of the grafted monomer. This indicated that the smaller the molecule was, the easier its grafting onto the PP chains was. GD was obtained from the FTIR spectra on the basis of a method described elsewhere.[18,21] The maximum GDs of PP-*g*-PEGMEMA$_{300}$, PP-*g*-PEGMEMA$_{475}$, and PP-*g*-PEGMEMA$_{1100}$ were 4.6, 3.8, and 2.5 wt %, respectively.

Figure 4 shows the representative ^{1}H-NMR spectrum of PP-*g*-PEGMEMA$_{300}$ with low molecular weight (residue 1). Clearly, the ^{1}H-NMR analysis provided evidence for the grafting reaction. Because the unsaturated α carbon in the CH_2=C(CH_3)COO— group should have been saturated with hydrogen to terminate the grafting reaction,[21] we could calculate the average degree of polymerization for the grafted chains ($\overline{X}_{n,g}$) on the basis of the methine hydrogen intensity in the —CH_2—C*H*(CH_3)COO— group:

$$\overline{X}_{n,g} = \frac{I_a + I_{a'} + I_a}{2I_g} \quad (1)$$

where $(I_a + I_{a'} + I_{a''})/2$ is one hydrogen intensity in the methylene of the —CH_2C(CH_3)COO— group and I_g is the hydrogen intensity in the methine of the —CH_2—C*H*(CH_3)COO— group. The physical properties of PEGMEMA and the corresponding graft copolymer, PP-*g*-PEGMEMA$_x$ (where *x* denotes the molecular weight of PEGMEMA), are presented in Table I.

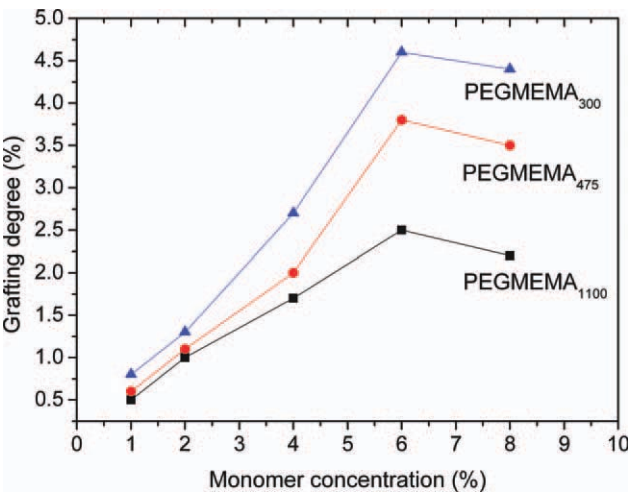

Figure 2 Grafting reactions as a function of the monomer concentration. [Color figure can be viewed in the online issue, which is available at wileyonlinelibrary.com.]

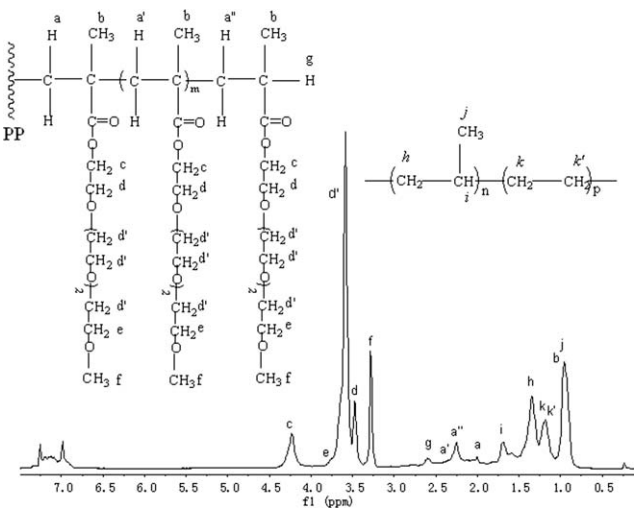

Figure 4 ^{1}H-NMR spectrum of PP-*g*-PEGMEMA$_{300}$.

TABLE I
Monomer Structures and Results of the Grafting Reactions onto PP

Monomer	Structure	GD (wt %)	$\overline{X}_{n,g}$
$PEGMEMA_{300}$	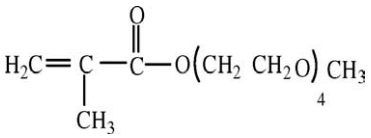	2.7	2.0
$PEGMEMA_{300}$	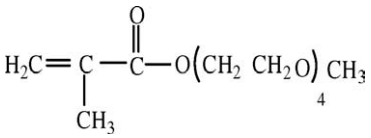	4.6	3.5
$PEGMEMA_{475}$	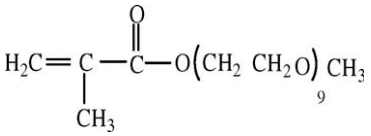	2.0	1.5
$PEGMEMA_{475}$	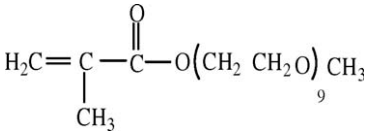	3.8	3.0
$PEGMEMA_{1100}$	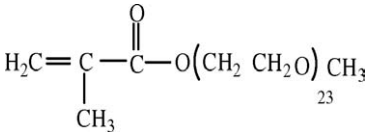	1.2	1.0
$PEGMEMA_{1100}$	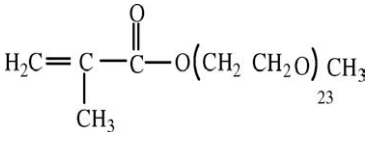	2.5	2.0

Surface properties of the spin-coated film

The results of the static water contact angle measurements on the surfaces of the spin-coated films of neat and grafted PP are shown in Figure 5. The static water contact angle on the surface of the neat PP film was 105.1° [Fig. 5(a)], in agreement with data reported for PP plates.[22] As PEGMEMA had a hydrophilic character, it was expected that the static water contact angle would decrease with increasing GD.[5,23] However, only a slight decrease in the water contact angle of the grafted samples was observed [Fig. 5(b–d)]; regardless of GD, the three grafted samples showed similar hydrophobicities (with contact angle values of about 97°). This result indicated that only small amounts of grafted PEGMEMA chains were located on the top layers of the graft copolymer surface.

Figure 6 shows the angular-dependent XPS spectra at two sampling depths (angle = 60°, ~ 3 nm; angle = 0°, ~ 10 nm) for the spin-coated film of PP-*g*-$PEGMEMA_{475}$. The sampling depth for the C_{1s} photoelectrons decreased from about 10 to 3 nm as the take-off angle increased from 0 to 60°.[5] The C_{1s} core-level peak position of the carbon atoms was approximately 284.5 eV, and the peak position for oxygen was centered around 532.5 eV.[24] To compare the content of oxygen atoms at different sampling depths, the peak intensity was normalized by the peak intensity of the carbon atom. Figure 7 shows the XPS depth profiling of the spin-coated films for the neat PP [Fig. 7(a)] and graft copolymer PP-*g*-$PEGMEMA_{475}$ [Fig. 7(b)], respectively. The oxygen atoms in the neat PP sample may have come from oxidation or contamination of the PP surface.[24] No difference in the oxygen content was observed at different positions along the sampling depth for the neat PP films. In contrast, the oxygen content for the PP-*g*-$PEGMEMA_{475}$ sample decreased with increasing take-off angle; this suggested that the grafted chains did not cover the topmost layer of the surface but distribute themselves in a gradient along the depth from the topmost layer.

This surface segregation analysis was governed by enthalpic factors.[25–27] As the surface energy (γ) of PEGMEMA was higher than that of the PP chains (γ_{PP} = 30 mN/m < γ_{PEG} = 43 mN/m),[28,29] PEGMEMA tended to be covered by PP chains to reduce the surface energy of the graft copolymer. Thus, the

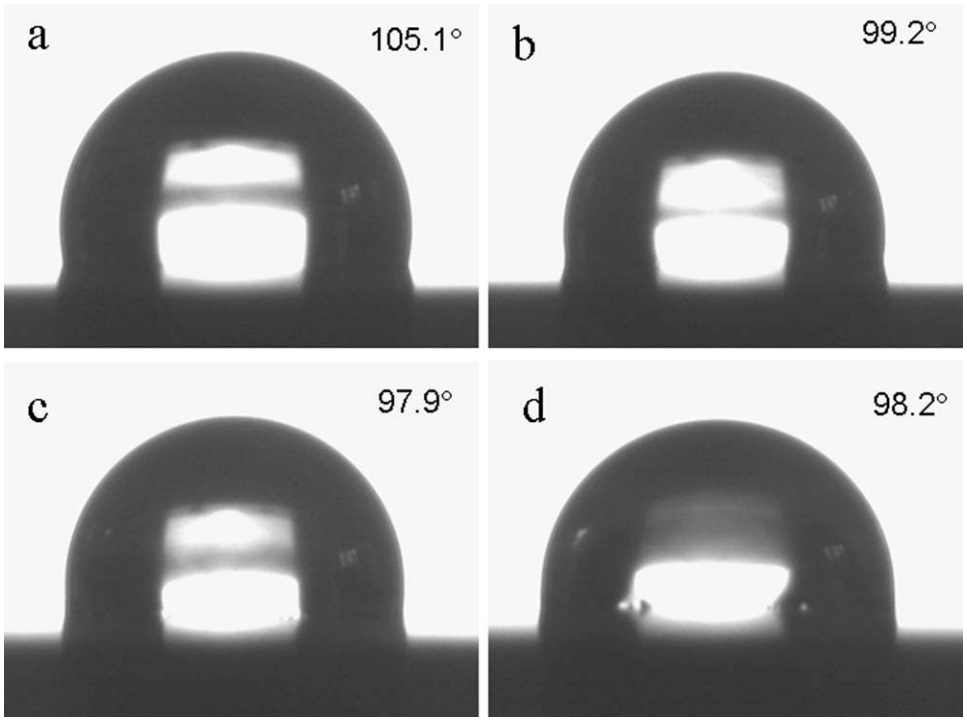

Figure 5 Water contact angle values on the surfaces of the neat and grafted PP: (a) neat PP, (b) PP-*g*-PEGMEMA$_{300}$ (GD = 4.8%), (c) PP-*g*-PEGMEMA$_{475}$ (GD = 3.8%), and (d) PP-*g*-PEGMEMA$_{1100}$ (GD = 2.5%).

oxygen content on the surface was lower than that simply calculated on the basis of GD. This was the reason that the surface hydrophilicity of the melt-grafted copolymer did not vary linearly with GD.[30]

Restructuring of the spin-coated film

To obtain a graft copolymer with a restructured surface enriched in PEGMEMA microdomains, the spin-coated films were annealed at 100°C for 4 h and then immersed in distilled water at 60°C for 24 h. The oxygen content at the surface, detected by XPS, was used to monitor the diffusion of PEGMEMA chains, and the water contact angle was used to characterize the wetting activity of the surface. The XPS detection was fixed at take-off angle of 60°, and at this take-off angle, the detected depth was estimated to be about 3 nm.[5,23] Thus, the XPS detection was assumed to detect the topmost layer of the graft copolymer.

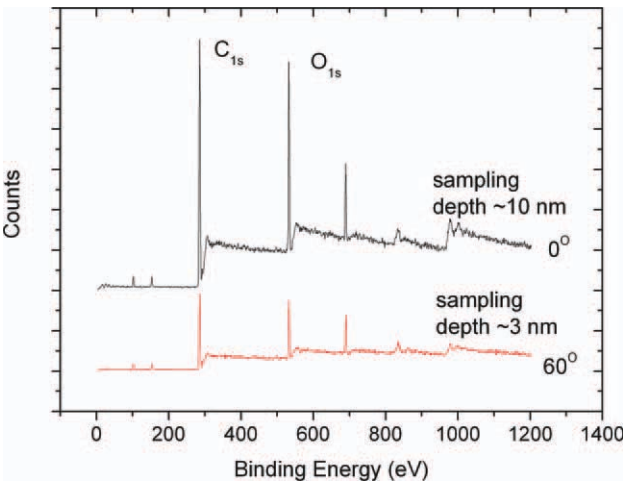

Figure 6 Angular-dependent XPS spectra at two sampling depths (angle = 60°, ~ 3 nm; angle = 0°, ~ 10 nm) for the spin-coated film of PP-*g*-PEGMEMA$_{475}$ (GD = 3.8%). [Color figure can be viewed in the online issue, which is available at wileyonlinelibrary.com.]

The XPS and water contact angle results of the spin-coated PP-*g*-PEGMEMA$_{475}$ film before and after treatment are shown in Figure 8. The oxygen content obtained from XPS was observed to decrease with annealing time; this indicated that annealing facilitated the microphase separation, and grafted PEGMEMA tended to deplete from the topmost layer.[5,17] Correspondingly, the water contact angle increased from 98 to 102°. After the sample was immersed in water for 24 h, the oxygen content ([O]/[C]) increased from 33 to 71%. The water contact angle decreased correspondingly from 102 to 78°; this indicated that surface rearrangement occurred, and more PEGMEMA was induced to enrich the topmost layer of the surface by PEGMEMA–water interaction.

The surfaces of the treated films were examined by noncontact mode AFM. The surface morphology is shown in Figure 9. The spin-coated film showed isolated dark domains dispersed in a bright matrix [Fig. 9(a)]. On the basis of the composition of grafted

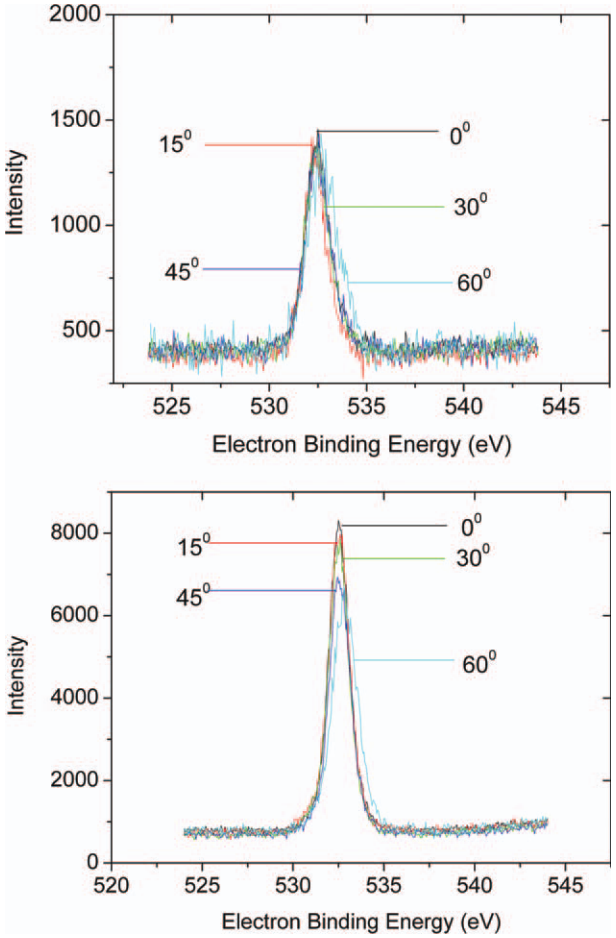

Figure 7 Depth-dependent XPS results for the spin-coated films: (a) neat PP and (b) PP-*g*-PEGMEMA$_{475}$ (GD = 3.8%). [Color figure can be viewed in the online issue, which is available at wileyonlinelibrary.com.]

PP, the bright and dark areas in the image were assigned to the PP matrix and PEGMEMA cylinders, respectively. The dark spherical domains decreased

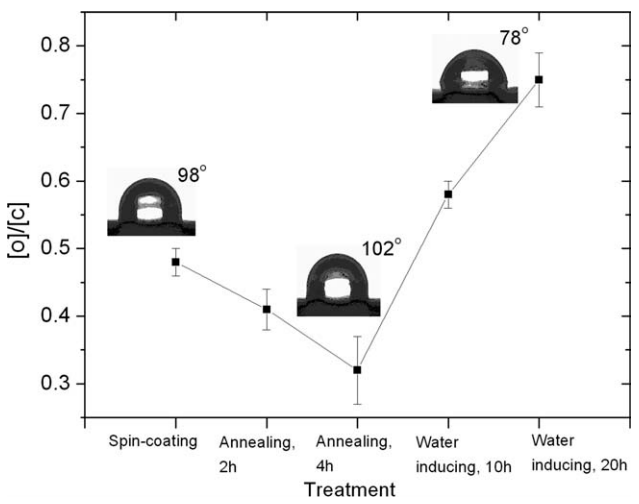

Figure 8 XPS and water contact angle results of the spin-coated PP-*g*-PEGMEMA$_{475}$ film before and after treatment.

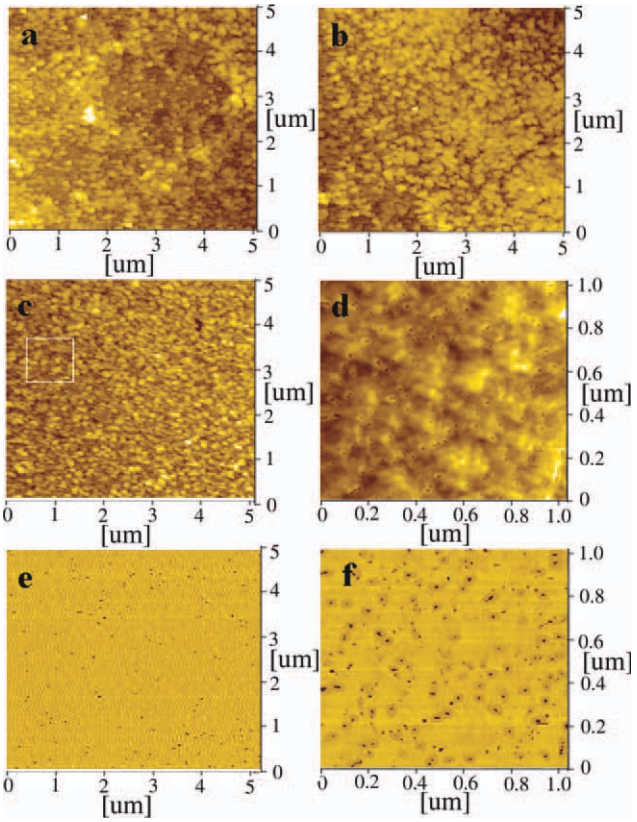

Figure 9 AFM images of the spin-coated PP-*g*-PEGMEMA$_{475}$ film before and after treatment: (a) height image of the as-prepared film, (b) height image of the film annealed for 4 h, (c) height image of the film after solvent induction for 24 h, (d) height image of an enlarged area of part c, (e) phase image of part c, and (f) phase image of part d. [Color figure can be viewed in the online issue, which is available at wileyonlinelibrary.com.]

after the sample was annealed for 4 h [Fig. 9(b)]; this indicated that the topmost surface of the graft copolymer was covered by the lower surface energy component, PP, at equilibrium after annealing. A hole-with-rim pattern was observed after sample induction by water for 24 h [Fig. 9(c)]. The holes were shown to be similar in their sizes, that is, 15–20 nm in diameter and 5–10 nm in depth [Fig. 9(d)]. The hole-with-rim structure was observed in an initial stage of a dewetting process, when a thin liquid layer on a solid substrate became unstable to rupture itself.[17,31] The dewetting process continued, accompanied by an enlarging of hole size and a grouping of rims to form two-dimensional foams, with subsequent breakup of the walls of the foam into isolated droplets. The restructured structure is shown in Figure 9(e). The phase separation was clearly detectable from the phase image of an enlarged area [Fig. 9(f)]. The covalent bonding between the grafted PEGMEMA chains and PP backbone led to microphase segregation (0.05–0.1 um).[31] The phase separation in the thin film of the graft copolymer restructured the film surface and resulted in a low water contact

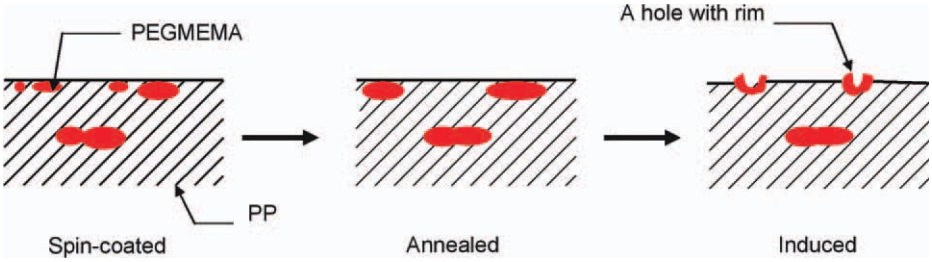

Figure 10 Schematic picture of the response to the treatments on the surface of PP-*g*-PEGMEMA$_{475}$. [Color figure can be viewed in the online issue, which is available at wileyonlinelibrary.com.]

angle (78°). As shown in Figure 10, the topmost PP layer on the studied graft copolymer surfaces likely underwent dewetting by immersion into water. The thin PP layers became unstable up to their rupture to form a hole-with-rim structure. The dewetting process was further promoted by the surface swelling of the PEGMEMA domains. In addition, the dewetting process was hindered by geometric confinement of the PP segment covalently linked to the PEGMEMA segment. Because the formation of the PEGMEMA–water interface was the major driving force for the surface rearrangement process, the holes-with-rims were easily covered by the grafted PEGMEMA component, and the restructured structure on the PP-*g*-PEGMEMA graft copolymer formed a hydrophilic surface.

This result was very important because it demonstrated the possibility of modifying bulk materials through melt grafting and posttreatment to improve their biocompatibility. It is worth noting that the formation of the hole-with-rim patterns was not observed for the homologous PP-*g*-PEGMEMA$_{300}$ and PP-*g*-PEGMEMA$_{1100}$ samples after annealing and water treatment; this indicated that both GD and the length of the grafted chains substantially affected the surface restructuring. On the basis of thermodynamic theory for microphase separation of diblock copolymers, the equilibrium morphologies were determined by the copolymer composition and the segregation degree (χN) between the two blocks.[32] Similarly, the equilibrium morphologies of random grafting copolymer (RGC) depended on GD and χN, where χ is the Flory–Huggins segment–segment interaction parameter and N is the degree of polymerization.[10,11] In the case of PP-*g*-PEGMEMA, N was the sum of the average number of propylene repeating units between two consecutive PEGMEMA grafts and the number of monomeric units in one PEGMEMA graft. χ is a temperature-dependent parameter and is constant at a specific temperature, and N is mainly dependent on GD. That is, a relatively high GD ensured relatively short PP segments between two graft points and microscopic heterogeneities in the composition at a length scale comparable to the molecular dimensions.[9] This favored microphase separation. At the same time, long graft chains increased the probability of interaction between water and PEGMEMA. In our study, GD for PP-*g*-PEGMEMA$_{475}$ was no less than 3.8 wt %, and the length of the grafted chains was no less than 42 carbons. These were the conditions under which microphase separation could be observed.

Biocompatibility of the restructured surface

It was reported that when a foreign surface contacts blood, the initial response is blood-protein adsorption on the surface, followed by platelet adhesion and activation of coagulation pathways, which lead to thrombus formation.[33] Therefore, protein adsorption on the investigated surfaces was tested to evaluate the biocompatibility of the graft copolymer. Herein, BSA (concentrations of BSA = 1.0 and 2.0 mg/mL) was used as a model protein. The protein adsorption on the surfaces of the neat PP and PP-*g*-PEGMEMA$_{475}$ films with and without treatment is shown in Figure 11. Because of its hydrophobicity, the neat PP film was found to exhibit the

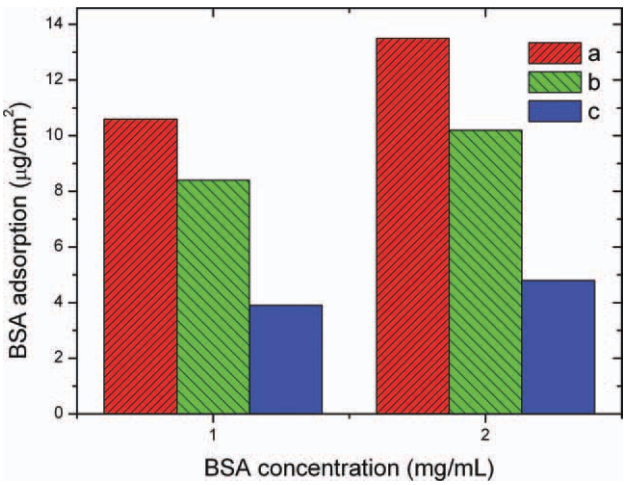

Figure 11 Dependence of the BSA adsorption on the film surface for different BSA concentrations: (a) neat PP, (b) PP-*g*-PEGMEMA$_{475}$ without treatment, and (c) PP-*g*-PEGMEMA$_{475}$ after treatment. [Color figure can be viewed in the online issue, which is available at wileyonlinelibrary.com.]

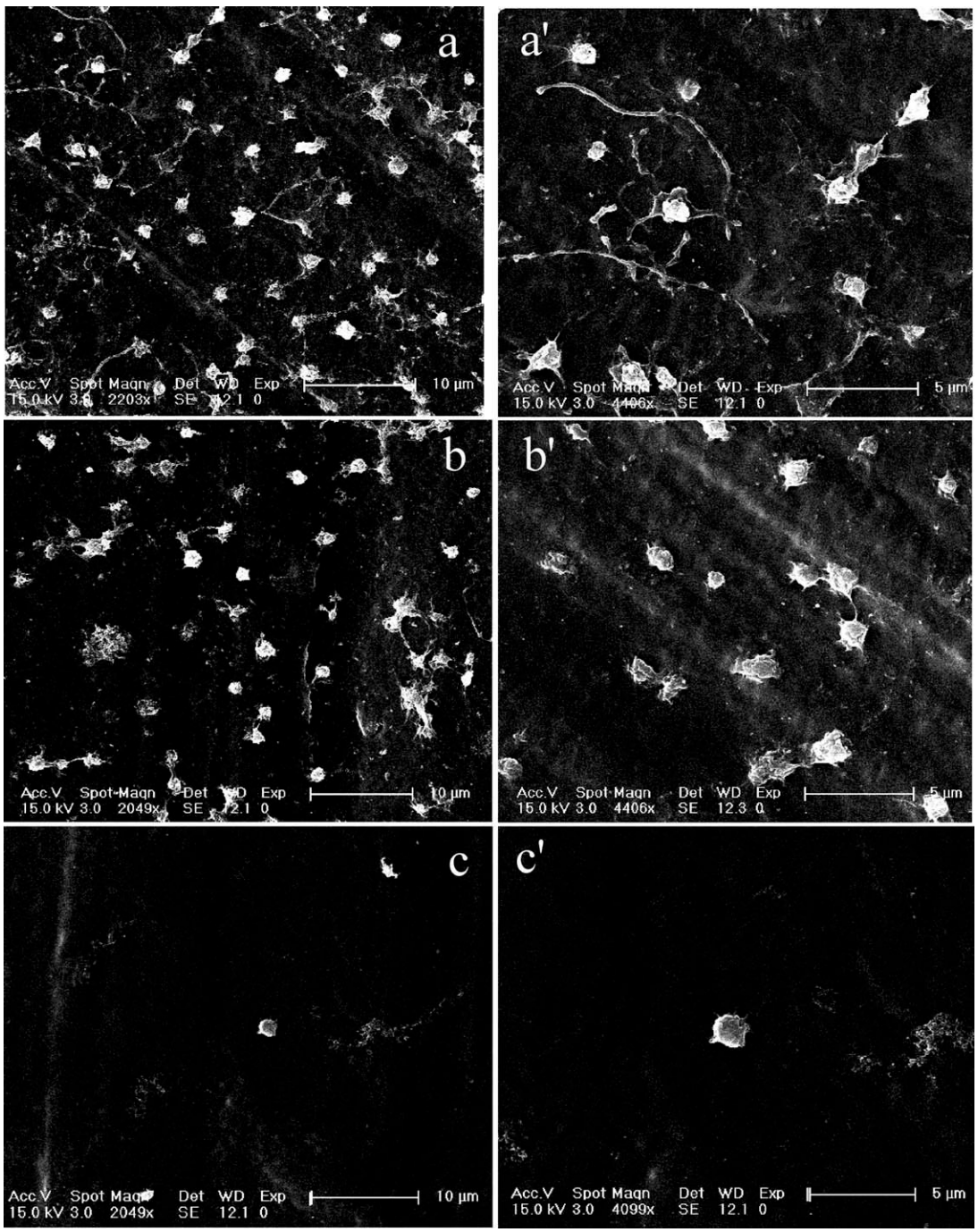

Figure 12 SEM pictures of platelet adhesion on the surfaces of the neat PP and PP-*g*-PEGMEMA films: (a) neat PP, (a′) enlarged area of part a, (b) PP-*g*-PEGMEMA without treatment, (b′) enlarged area of part b, (c) PP-*g*-PEGMEMA after treatment, and (c′) enlarged area of part c.

highest BSA adsorption. The adsorption amounts were 10.6 and 13.5 μg/cm^2 in 1.0 and in 2.0 mg/mL BSA solutions, respectively. Decreased BSA adsorption was observed on the PP-*g*-PEGMEMA$_{475}$ film without treatment (8.4 μg/cm^2 in the 1.0 mg/mL BSA solution and 10.2 μg/cm^2 in the 2.0 mg/mL BSA solution). In contrast, the average amounts of BSA adsorption on the PP-*g*-PEGMEMA$_{475}$ film after treatment were 3.9 μg/cm^2 in the 1.0 mg/mL BSA solution and 4.8 μg/cm^2 in the 2.0 mg/mL BSA solution; this corresponded to about a 65% reduction in protein adsorption at the surface with respect to the neat PP film. These results demonstrate that the graft copolymers with restructured surfaces (enrichment of PEGMEMA on the topmost layer) possessed high biocompatibility.[33,34]

SEM images of the platelets adhered on the neat PP and PP-*g*-PEGMEMA$_{475}$ films with and without

treatment after 60 min of incubation are shown in Figure 12. For the neat PP film [Fig. 12(a)], a great number of platelets were attached to the surface, and most of them had extended pseudopodia [Fig. 12(a′)]. The adhesion of platelets on the surface of PP-*g*-PEGMEMA$_{475}$ without treatment was only slightly diminished [Fig. 12(b,b′)]. The platelet adhesion was substantially decreased on the surface of PP-*g*-PEGMEMA$_{475}$ after water treatment. A negligible amount of nonactivated platelets were attached as disk-shaped cells typically from 2 to 5 μm across [Fig. 12(c,c′)]. Note that the water contact angle on PP-*g*-PEGMEMA$_{475}$ with treatment was 78°, nearly within the moderate ($55° < \theta < 75°$) water contact angle range at which the surface exhibits minimal activation of blood–plasma coagulation through the intrinsic pathway.[35] The overall results provide evidence that the restructured surfaces of the copolymer enriched in PEGMEMA chains possessed high biocompatibility.

CONCLUSIONS

We demonstrated that highly biocompatible PP could be prepared by melt grafting and water-induced surface restructuring. A hydrophilic monomer, PEGMEMA, was melt-grafted onto PP backbones, and films of the grafted copolymers were treated by distilled water. The formation of hole-with-rim patterns and the enrichment of PEGMEMA chains on the topmost surface were key factors for the observed improved biocompatibility. The GD and length of grafted chains were important parameters in the control of the surface restructuring process. The method proposed here allows, in general, for the possibility of creating a highly controlled surface coverage of a hydrophobic substrate by higher energy polymer chains linked via melt grafting. It also advances graft copolymers generated through melt grafting as new candidates for applications not only in the field of blood-contact materials and devices but also for biomedical implants requiring good hydrophilicity and protein adsorption resistance.

This work was carried out in the framework of a Research Cooperation Agreement between the Chinese Academy of Sciences and the National Research Council of Italy. The authors thank the reviewers for their constructive comments on this article.

References

1. Colman, R. W.; Scott, C. F.; Schaier, A. H.; Wachtfogel, Y. T.; Pixley, R. A.; Edmunds, L. H. In Blood in Contact with Natural and Artificial Surfaces; Leonard, E. F., Turitto, V. T., Vroman, L., Eds.; Annals of the New York Academy of Sciences: New York, 1987; p 516.
2. Andersen, T. E.; Palarasah, Y.; Skjødt, M.; Ogaki, R.; Benter, M.; Alei, M.; Hans Kolmos, H. J.; Koch, C.; Kingshott, P. Biomaterial 2011, 32, 4481.
3. Faxälv, L.; Ekblad, T.; Liedberg, B.; Lindahl, T. L. Acta Biomater 2010, 6, 2599.
4. Michel, V. Prog Polym Sci 2007, 32, 755.
5. Kingshott, P.; Thissen, H.; Griesser, H. J. Biomaterials 2002, 23, 2043.
6. Blümmel, J.; Perschmann, N.; Aydin, D.; Drinjakovic, J.; Lopez-Garcia, M.; Kessler, H.; Spatz, J. P. Biomaterials 2007, 28, 4739.
7. Wang, P.; Tan, K. L.; Ho, C. C.; Khew, M. C.; Kang, E. T. Eur Polym J 2000, 36, 1323.
8. Badel, T.; Beyou1, E.; Bounor-Legarél, V.; Chaumont, P.; Flat, J. J.; Michel, A. J Polym Sci Part A: Polym Chem 2007, 45, 5215.
9. Passaglia, E.; Coiai, S.; Augier, S. Prog Polym Sci 2009, 34, 911.
10. Mark, P. R.; Murthy, N. S.; Weigand, S.; Breitenkamp, K.; Kade, M.; Emrick, T. Polymer 2008, 49, 3116.
11. Zhang, L.; Lin, J.; Lin, S. J Phys Chem B 2008, 112, 9720.
12. Patel, D. M.; Fredrickson, G. H. Phys Rev E 2003, 68, 051802.
13. Mihaylova, M. D.; Krestev, V. P.; Kresteva, M. N.; Amzil, A.; Berlinova, I. V. Eur Polym J 2001, 37, 233.
14. Qi, S.; Chakraborty, A. K.; Wang, H.; Lefebvre, A. A.; Balsara, N. P.; Shakhnovich, E. I.; Xenidou, M.; Hadjichristidis, N. Phys Rev Lett 1999, 82, 2896.
15. Eitouni, H. B.; Rappl, T. J.; Gomez, E. D.; Balsara, N. P.; Qi, S.; Chakaborty, A. K.; Fréchet, J. M. J.; Pople, J. A. Macromolecules 2004, 37, 8487.
16. Huang, Z.; Chen, M.; Pan, S.; Chen, D. Biomed Mater 2010, 5, 054116.
17. Pientka, Z.; Oike, H.; Tezuka, Y. Langmuir 1999, 15, 3197.
18. Cai, C.; Shi, Q.; Li, L.; Zhu, L.; Yin, J. Radiat Phys Chem 2008, 77, 370.
19. Yang, Q.; Xu, Z. K.; Dai, Z. W.; Wang, J. L. Chem Mater 2005, 17, 3050.
20. Demirel, G.; Özçetin, G.; Turan, E.; Çaykara, T. Macromol Biosci 2005, 5, 1032.
21. Shi, Q.; Zhu, L.; Cai, C.; Yin, J.; Costa, G. Polymer 2006, 47, 1979.
22. Tao, G.; Gong, A.; Lu, J.; Sue, H.; Bergbreiter, D. Macromolecules 2001, 34, 7672.
23. Winter, R.; Nixon, P. G.; Gard, G. L.; Castner, D. G.; Holcomb, N. R.; Hu, Y.-H.; Grainger, D. W. Chem Mater 1999, 11, 3044.
24. Ishihara, K.; Iwasaki, Y.; Ebihara, S.; Shindo, Y.; Nakabayashi, N. Colloids Surf B 2000, 18, 325.
25. Menelle, A.; Russell, T. P.; Anastasiadis, S. H.; Satija, S. K.; Majkrzak, C. F. Phys Rev Lett 1992, 68, 67.
26. Kim, S. O.; Solak, H. H.; Stoykovich, M. P.; Ferrier, N. J.; de Pablo, J. J.; Nealey, P. F. Nature 2003, 424, 411.
27. Hu, S.; Brittain, W. J.; Solomon, J. S.; Balazs, A. C. Eur Polym J 2006, 42, 2045.
28. Shimizu, R. N.; Demarquette, N. R. J Appl Polym Sci 2000, 76, 1831.
29. Lin, Z.; Kim, D. H.; Wu, X.; Boosahda, L.; Stone, D.; LaRose, L.; Russell, T. P. Adv Mater 2002, 14, 1372.
30. Xin, Z.; Ding, Y.; Yin, J.; Ke, Z.; Xu, X.; Gao, Y.; Costa, G. J Polym Sci Part B: Polym Phys 2005, 43, 314.
31. Muller-Buschbaum, P.; Stamm, M. Macromolecules 1998, 31, 3686.
32. Bates, F. S. Science 1991, 251, 898.
33. Cheng, H.; Yuan, L.; Song, W.; Wu, Z.; Li, D. Prog Polym Sci 2008, 33, 1059.
34. Werner, C.; Maitz, M. F.; Sperling, C. J Mater Chem 2007, 17, 3376.
35. Golas, A.; Parhi, P.; Dimachkie, Z. O.; Siedlecki, C. A.; Vogler, E. A. Biomaterials 2010, 31, 1068.